PEERING INTO THE NON-PERTURBATIVE PHASE-SPACE REGIONS OF JETS*

Liliana Apolinário, Nuno Olavo Madureira

Laboratório de Instrumentação e Física Experimental de Partículas (LIP)
Universidade de Lisboa — Instituto Superior Técnico (IST), Lisboa, Portugal

Raghav Kunnawalkam Elayavalli

Vanderbilt University, USA

Received 25 March 2024, accepted 27 August 2024, published online 15 October 2024

The study of Quantum Chromodynamics (QCD) at ultra-relativistic energies can be performed in a controlled environment through lepton–hadron deep inelastic scatterings (DIS), as in the future Electron Ion Collider (EIC). In such collisions, the high-energy QCD emissions that follow the ejection of hard partons are accurately described by perturbation theory. However, the lower-energy scales at which quarks and gluons experience colour confinement — hadronization — fall out of the validity regions for perturbative calculations, requiring phenomenological models to describe it. As such, hadronization physics cannot be currently derived from first principles alone. The Monte Carlo (MC) event generators are useful tools to describe these processes as they simulate both the perturbative (pQCD) and the non-perturbative (npQCD) interactions, with a model-dependent energy scale at which parton dynamics transition from one to the other. This work aims to use jets — experimental reconstructions of final-state particles likely to have a common partonic origin — to inspect this transition further. Although originally proposed to circumvent hadronization effects, we show that jets have great potential as probes of non-perturbative phenomena. The charge correlation ratio was recently shown to be sensitive to hadronization effects and our work shows that jet substructure selections, namely on formation time and the depth in the clustering tree at which the leading charged particles are resolved, can improve this sensitivity.

DOI:10.5506/APhysPolBSupp.17.6-A8

* Presented at *Excited QCD 2024*, Benasque, Huesca, Spain, 14–20 January, 2024.

1. Introduction

The production of asymptotically free partons in hard scattering collisions at high-energy scales, followed by their colour confinement into hadrons at low-energy scales, denote characteristic features of QCD which can be understood through the running of the α_s coupling constant. This transition from the elementary to the composite particles is the so-called hadronization process, which holds interest due to the current lack of a first-principled understanding of the underlying mechanics. For high-energy transfer processes, α_s is small, therefore allowing parton dynamics to be fully described by perturbative QCD. In this framework, highly-virtual partons emit gluons or split into quark–antiquark pairs by virtue of being asymptotically free. These parton branchings can be calculated first at tree level and have higher-order corrections to be introduced via the parton shower description, such as the ones implemented in the Monte Carlo (MC) event generators. However, for small energy scales, including the hadronization ones, α_s becomes prohibitively large and tightly binds the partons together, forming hadrons. Hence, the treatment of hadronization has to reflect the non-perturbative conversion of the coloured, outgoing final-state partons into colourless hadrons through a combination of analytical results and different QCD-based phenomenological models. There are two main classes of hadronization models — the Lund string [1, 2] and the cluster fragmentation [3] approaches, implemented in the PYTHIA [4, 5] and Herwig [6] MC event generators, respectively.

2. Deep Inelastic Scattering and jet reconstruction

Vacuum Deep Inelastic Scatterings (DIS) provide a clean environment to study the hadronization mechanism and confinement dynamics, as they produce final states with typically low multiplicities, allowing for more precise measurements. As such, the modifications from vacuum to nuclear DIS events can help us understand the space-time evolution preceding the final-state hadrons, including the timescales of the hadronization process. DIS features are also needed to test and calibrate the theoretical tools, such as the MC event generators, that are used to study the quark–gluon plasma produced in heavy-ion collisions. To recover the initial momentum of the hard scattered partons produced in vacuum DIS, the particle output of the event can be arranged into jets [7]. A jet is a highly-collimated group of hadrons likely to have the same partonic origin, structured to recover the initial energy degraded by the boosted, angular-ordered branching sequence. Using the kinematic information of the jet's constituents, the particle grouping is ordered — clustering sequence, providing a proxy for the particle evolution

history via the jet-fragmentation pattern — clustering tree. Although originally proposed to circumvent hadronization effects, we show that jets have sensitivity, via their substructure, to non-perturbative phenomena.

We simulated 10 million DIS electron–proton collisions using both PYTHIA 8 and Herwig 7 with beam energies of $\sqrt{s_e} = 18$ GeV and $\sqrt{s_p} = 275$ GeV for the electrons and protons, respectively. A minimum momentum transfer of $Q^2 > 50$ GeV^2 is imposed on the simulations and particles are selected with transverse momentum $p_{\mathrm{T}} > 200$ MeV/c. For each event, jets are identified with the anti-k_{T} [8] clustering algorithm, with the jet radius set to $R = 1$. Then, the event's jets are re-clustered using the Cambridge/Aachen (C/A) [9] algorithm for the subsequent jet substructure studies. Jets are selected with $p_{\mathrm{T,jet}} > 5$ GeV/c and pseudorapidity $-1.5 < \eta_{\mathrm{jet}} < 3.5$. Finally, the jets are also groomed with the soft-drop (SD) algorithm [10], allowing for a crisper separation between the perturbative and non-perturbative portions of the clustering trees. Setting the soft threshold $z_{\mathrm{cut}} = 0.1$ and the angular exponent $\beta = 0$, the SD criterion in Eq. (1)

$$\frac{\min\left(p_{\mathrm{T1}}, p_{\mathrm{T2}}\right)}{p_{\mathrm{T1}} + p_{\mathrm{T2}}} > z_{\mathrm{cut}} \left(\frac{\Delta R_{12}}{R}\right)^{\beta} \tag{1}$$

requires jet splittings to have a momentum fraction greater than 0.1, where $\Delta R_{12}^2 = (y_1 - y_2)^2 + (\phi_1 - \phi_2)^2$, $y_{1(2)}$ the rapidity of particle 1(2) and $\phi_{1(2)}$ its azimuthal angle.

With the goal of comparing hadronization models in mind, we select the parton shower descriptions in PYTHIA and Herwig that produce the best agreement between the particle and jet ϕ, η, and p_{T} distributions from both MC. For the chosen collision settings, the results matched the most for the PYTHIA Dire shower and the Herwig default shower approach. The C/A clustering trees are declustered step by step until the following three splittings of interest are found — the Leading Charged Particles splitting (LCP, Fig. 1, red/light grey particles), the resolved soft-drop splitting (RSD, Fig. 1, red/light grey splitting) and the first soft-drop (1SD, Fig. 1, blue/grey splitting). By construction, the LCP factors the features of the 2 leading charged particles from a jet and will be mostly sensitive to the phenomena taking place at the latest stages of the jet-fragmentation pattern, where non-perturbative effects, like hadronization, are dominant. While not a realistic splitting in a theoretical sense, the LCP is independent of clustering topologies. In order to have a gauge on how deep into the jet-fragmentation pattern did the LCP get resolved at, the RSD is defined as the soft-drop approved unclustering step, where the 2 leading charged particles are resolved into independent subjets. Finally, to have a well-established benchmark for the jet substructure studies, we also account for the 1SD, as it is the first

de-clustering step starting from the fully clustered jet that yields the DGLAP splitting functions predicted by pQCD. All analysis steps were performed using the FastJet package [11].

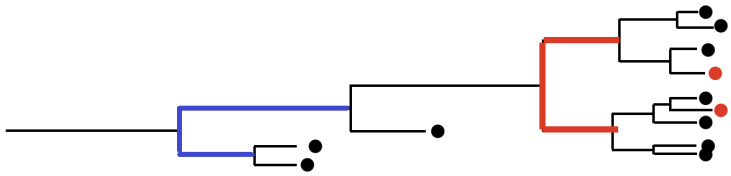

Fig. 1. (Colour on-line) Leading charged particles (LCP) in red/light grey circles, resolved soft-drop splitting (RSD) in the red/light grey splitting, and first soft-drop splitting (1SD) in the blue/grey splitting.

3. Charge correlation ratio

Taking the differential cross sections for the production of jets with equally-charged, $\mathrm{d}\sigma_{hh}/\mathrm{d}X$, and oppositely-charged, $\mathrm{d}\sigma_{h\bar{h}}/\mathrm{d}X$, leading charged hadrons of flavour $h = \pi^+, K, p$, the charge correlation ratio [12] is defined as

$$r_{\mathrm{c}}(X) = \frac{\mathrm{d}\sigma_{hh}/\mathrm{d}X - \mathrm{d}\sigma_{h\bar{h}}/\mathrm{d}X}{\mathrm{d}\sigma_{hh}/\mathrm{d}X + \mathrm{d}\sigma_{h\bar{h}}/\mathrm{d}X}\,, \tag{2}$$

with respect to a given jet substructure variable X. Therefore, r_{c} acts as a measure of the probability of producing jets with a given charge configuration of their LCP: positive r_{c} means a greater probability of jets having both positive or both negative LCP, while negative r_{c} signals that jets tend to have both positive and negative leading charges.

For X, we will consider the formation time τ_{form} [13], which is the time that a quantum state, such as a parton, takes to behave as two independent sources of additional radiation, like the two daugther-partons from a splitting. For a jet splitting, τ_{form} can be calculated by [14]

$$\tau_{\mathrm{form}} = \frac{1}{2\,E\,z\,(1-z)\;(1-\cos\theta_{12})}\,, \tag{3}$$

where $E = E_1 + E_2$ is the total energy, E_1 and E_2 the daughters' energies, θ_{12} the opening angle between the daughters' 3-momenta, and $z = \min(E_1, E_2)\,/\,(E_1 + E_2)$ is the energy fraction.

The charge-ratio dependence of the LCP formation time for jets with leading pions, kaons, and protons is shown in Fig. 2, left panel [12]. For large $\tau_{\mathrm{form,LCP}}$, the charge ratios are approximately stable around fixed negative values. This reveals a strong preference towards the production of

opposite LCPs, as jets with late LCP are less likely to have subsequent splittings randomizing the correlation between the charges. However, for small $\tau_{\mathrm{form,LCP}}$, the charge ratios become significantly closer to zero, highlighting a randomization of the LCP charge profile.

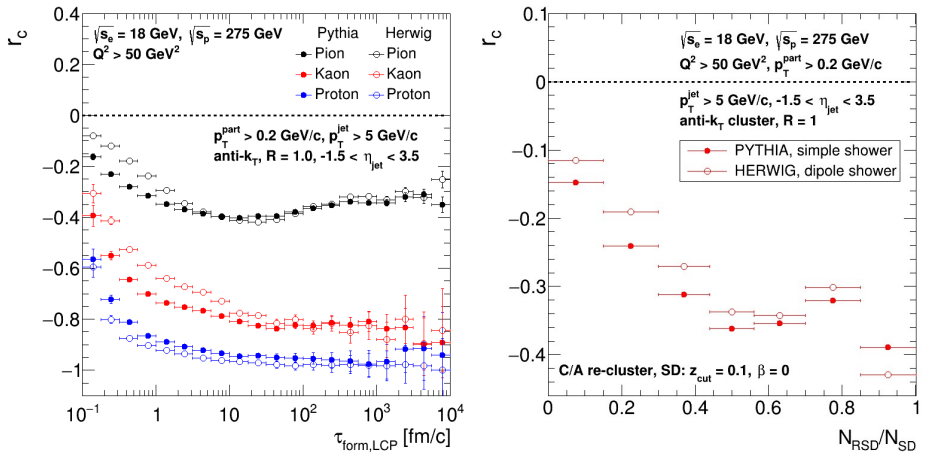

Fig. 2. (Colour on-line) Left: charge ratios with respect to the LCP formation time for jets with leading charged pions, kaons, and protons, represented in the black, red/light grey, and blue/grey circle markers, respectively, where full circles are used for PYTHIA ratios and open circles for Herwig. Right: charge ratios with respect to the RSD depth.

To have a gauge on how different jet-fragmentation patterns are contributing to this r_c behaviour, we study the charge ratio with respect to the RSD depth, given by the ratio between the splitting number of the RSD and the total number of SD splittings along the main jet branch, $N_{\mathrm{RSD}}/N_{\mathrm{SD}}$. In the right panel of Fig. 2, the explicit substructure-dependence of the r_c is showcased, with the charge ratios closest to zero coming from the jets whose RSD is taking place at the earliest stages of the clustering trees. After $N_{\mathrm{RSD}}/N_{\mathrm{SD}} \approx 0.5$, the r_c plateaus on highly-negative values, indicating that jets with late-stage RSD will strongly preserve an opposite-charge relation for their LCP.

Using these observations, Fig. 3 replicates the results from the left panel of Fig. 2, but this time selecting separately the jets with early RSD ($N_{\mathrm{RSD}}/N_{\mathrm{SD}} < 0.5$), shown in the left panel, and the jets with late RSD ($N_{\mathrm{RSD}}/N_{\mathrm{SD}} > 0.5$), shown in the right panel. While the $N_{\mathrm{RSD}}/N_{\mathrm{SD}} < 0.5$ selection maintains a similar qualitative behaviour between the PYTHIA and Herwig r_c dependence with respect to formation time, $N_{\mathrm{RSD}}/N_{\mathrm{SD}} > 0.5$ is revealing significant discrepancies for small $\tau_{\mathrm{form,LCP}}$ jets. PYTHIA does not

have a significant dependence on $\tau_{\mathrm{form,LCP}}$, while for Herwig, there is a steep climb towards $r_{\mathrm{c}} = 0$ for early-time LCP jets. Since the r_{c} is mostly sensitive to the hadronization model and we tuned the partonic development of these MC to yield the same event, the differences observed come entirely from the hadronization models. As such, this selection allows to finally pinpoint discrepancies coming from the string model that retains the memory of the incoming parton on the LCP fragmentation, as opposed to the cluster model. In this case, for the small $\tau_{\mathrm{form,LCP}}$, there will be enough subsequent unclustering steps to randomize the resulting hadronization pattern.

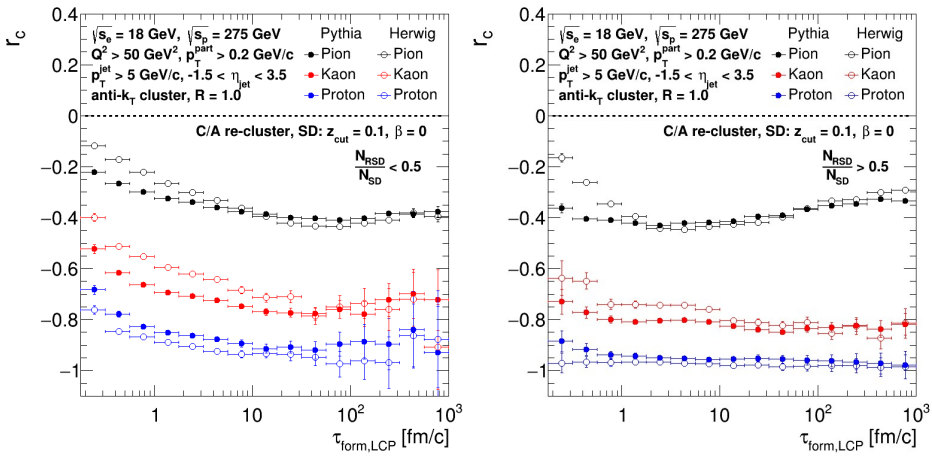

Fig. 3. (Colour on-line) Left: charge ratios with respect to the LCP formation time for early-RSD jets with leading charged pions, kaons, and protons, represented in the black, red/light grey, and blue/grey circle markers, where full circles are used for PYTHIA ratios and open circles for Herwig. Right: the same plot for late-RSD jets (the same marker scheme).

4. Conclusions

This work uncovers an explicit dependence of the charge correlation ratio on the topology of the jet-fragmentation pattern. This was achieved through the introduction of the RSD and checking the r_{c} dependence on the RSD depth in the jet. Namely, a selection based on the RSD depth reveals a qualitatively different behaviour between the charge ratios predicted by PYTHIA and Herwig, magnifying the sensitivity of this variable to the hadronization physics described by the two models — Lund string and cluster fragmentation.

This work was supported by the European Research Council (ERC) projects ERC-2018-ADG-835105 YoctoLHC and ERC-2018-STG-803183 CollectiveQCD; by OE Portugal, Fundação para a Ciência e a Tecnologia (FCT), I.P., projects EXPL/FIS-PAR/0905/2021 and CERN/FIS-PAR/0032/2021. N.O.M. acknowledges the financial support by FCT under Ph.D. grant PRT/BD/154611/2022.

REFERENCES

[1] B. Andersson, G. Gustafson, B. Söderberg, *Z. Phys. C* **20**, 317 (1983).

[2] T. Sjöstrand, *Nucl. Phys. B* **248**, 469 (1984).

[3] D. Amati, G. Veneziano, *Phys. Lett. B* **83**, 87 (1979).

[4] C. Bierlich *et al.*, *SciPost Phys. Codeb.* **2022**, 8 (2022).

[5] T. Sjostrand *et al.*, *J. High Energy Phys.* **2006**, 026 (2006)

[6] M. Bahr *et al.*, *Eur. Phys. J. C* **58**, 639 (2008).

[7] G. Salam, *Eur. Phys. J. C* **67**, 637 (2010).

[8] M. Cacciari, G.P. Salam, G. Soyez, *J. High Energy Phys.* **2008**, 063 (2008).

[9] Y.L. Dokshitzer, G.D. Leder, S. Moretti, B.R. Webber, *J. High Energy Phys.* **9708**, 001 (1997).

[10] A.J. Larkoski *et al.*, *J. High Energy Phys.* **2014**, 146 (2014).

[11] M. Cacciari, G.P. Salam, G. Soyez, *Eur. Phys. J. C* **72**, 1896 (2012).

[12] Y.-T. Chien *et al.*, *Phys. Rev. D* **105**, L051502 (2022).

[13] Y.L. Dokshitzer *et al.* (Eds.) «Basics of Perturbative QCD», *Fong and Sons Printers Pte. Ltd*, 1991.

[14] L. Apolinário, A. Cordeiro, K. Zapp, *Eur. Phys. J. C* **81**, 561 (2021).